Available online at www.sciencedirect.com
ScienceDirect
Journal of Power Sources 162 (2006) 579–588
JOURNAL OF POWER SOURCES
www.elsevier.com/locate/jpowsour

A study of the surface properties and steam reforming catalytic activity of nickel powders impregnated by *n*-alkanethiols

S. Rakass [a], H. Oudghiri-Hassani [a], N. Abatzoglou [b], P. Rowntree [a,*]

[a] *Département de Chimie, Université de Sherbrooke, 2500 Boul. Université, Sherbrooke, Quebec, Canada J1K 2R1*
[b] *Département de Génie Chimique, Université de Sherbrooke, 2500 Boul. Université, Sherbrooke, Quebec, Canada J1K 2R1*

Received 30 May 2006; received in revised form 30 June 2006; accepted 30 June 2006
Available online 20 September 2006

Abstract

The surface properties and catalytic activity of nickel powders impregnated with *n*-alkanethiols ($H–(CH_2)_n–SH$, $n = 4$, 5, 6, and 10) for the steam reforming of methane have been studied. The quantity and state of carbon and sulfur on fresh and used thiol-contaminated Ni catalysts were determined using XPS. The high catalytic activity and stability of $Ni–C_4S$ and $Ni–C_5S$ catalysts were similar to those of pristine Ni catalysts. However, the activity of $Ni–C_6S$ catalysts decreased for temperatures above ∼580 °C and no activity was obtained over the $Ni–C_{10}S$ at any temperature. Catalytic deactivation was principally caused by high surface coverages of aromatic carbon. The surface aromatic-carbon was due to the pyrolysis of the pre-adsorbed *n*-alkanethiols and not from the feed-gas methane. The aromatic carbon leads to the deactivation of the catalyst for the steam reforming of methane at coverages above ∼4.6%.

Keywords: Steam reforming; Unsupported Ni catalyst; *n*-Alkanethiols; Contamination; CH_4; Aromatic carbon

1. Introduction

The current abundance of natural gas is one of the key motivations of the continuing interest in conversion of methane to hydrogen. Steam reforming is an essential process in the manufacture of synthesis gas and hydrogen from hydrocarbons. The current steam reforming catalysts are mainly supported-nickel catalysts. However, coke formation [1–8] and sulfur poisoning [1,3,7,9,10] are two major problems associated with nickel catalysts. In fact, the sulfur compounds in gasoline and H_2S produced from these sulfur compounds in the hydrocarbon reforming process are poisonous to the reforming and shift catalysts in the fuel processor and the electrode catalysts in fuel cell stacks [11,12].

Deactivation of supported metal catalysts by carbon formation is another serious problem in steam reforming. Its causes are: (1) fouling of the metal surface, (2) blockage of catalyst pores and (3) loss of the structural integrity of the catalyst support material [1,3,4,7]. Carbon may be formed through different routes (mechanisms), which also determine the morphology of the carbon deposit. According to Rostrup-Nielsen et al. [1,7], three different kinds of carbon species are produced during steam reforming: (1) whisker-like carbon, (2) encapsulating carbon and (3) pyrolytic carbon. Whisker carbon is produced at temperatures above 450 °C by diffusion of carbon into nickel crystals, detachment of nickel from the support, and subsequent growth of whiskers with nickel on the top of the catalyst [1,4,5]. Pyrolytic carbon is usually created by thermal cracking of hydrocarbons above 600 °C [1,4,5] and deposition of carbon precursors, while encapsulating carbon is formed by slow polymerization of unsaturated hydrocarbons below 500 °C [1,4,5]. Both pyrolytic and encapsulating carbons cover the catalyst particle surface and therefore deactivate the catalyst. Although whisker carbon does not deactivate the catalyst directly, the accumulation of whisker carbon blocks the catalyst pores and increases the pressure drop in the reformers to unacceptable levels [1,4,5].

Sulfur is known to often inhibit chemical reactions [13–15] (poisoning) or change the selectivity (alter the product distribution) during catalytic reactions. Although sulfur is usually detrimental to the catalytic efficiency, a partial inhibition is some times desirable (e.g. carbon formation decrease during reforming). Sulfur and sulfur-bearing species are strongly chemisorbed

* Corresponding author. Tel.: +1 819 821 7006; fax: +1 819 821 8017.
E-mail address: Paul.Rowntree@USherbrooke.ca (P. Rowntree).

0378-7753/$ – see front matter © 2006 Elsevier B.V. All rights reserved.
doi:10.1016/j.jpowsour.2006.06.078

to most metal surfaces. The presence of sulfur on a catalyst surface usually causes substantial loss of activity in many reactions, particularly in methane steam reforming [1]. This loss of activity is due to: (1) sulfur adsorption on the nickel surface which prevents the further adsorption of reactant molecules, and (2) the reconstruction of Ni surface (i.e. sulfur can modify the chemical nature of the active sites or result in the formation of new compounds) which may modify or decrease the adsorption rates of reactant gases. The passivation effect of the adsorption of sulfur adatoms on transition metals seems to arise from the formation of a strong covalent bond between S and metal surfaces, which depletes the charge density of 'd' orbitals needed for the metal atoms to bind with other species. It has been shown that the adsorption of hydrogen sulphide on nickel catalyst is very strong at low temperatures and the fractional surface coverage depends on the value of P_{H_2S}/P_{H_2} [7,16,17]. In fact, dissociative adsorption of H_2S is very rapid with a sticking coefficient close to 1.0 for less than 70% of a full monolayer [7,10]. This suggests that there is no significant barrier to adsorption and dissociation until saturation of the surface is approached. In a study of sulfur adsorption on nickel, Alstrup and Andersen [18] have reported that the surface grid of sulfur did not coincide with the surface grid of the metal atoms (thus suggesting an incommensurate layer structure), although sulfur occupies a fourfold hollow site on Ni(1 0 0), independent of coverage. Adsorbed sulfur will deactivate nickel but also delineate ensembles of sites where sulfur is not adsorbed. Rostrup-Nielsen [9] suggested that the size of these ensembles was critical in allowing steam reforming with minimal formation of coke. Steam reforming is thought to involve ensembles of 3–4 nickel atoms, while carbon formation required six or seven atoms [9]. A complete coverage of the catalyst with sulfur results in total deactivation. However, at sulfur coverages of about 70% of saturation, carbon deposition could effectively be eliminated while the steam reforming reaction still proceeded [9]. Sulfur compounds are generally present in natural gas in the form of mixture of dimethyl disulfide and *tert*-butyl mercaptan (via deliberately added odourants [19]) and/or naturally present hydrogen sulphide. Much of the previous work focused on poisoning of nickel metal catalyst by H_2S but, there is no agreement in the literature regarding the effect of poisoning by organothiol on the catalytic activity during the steam reforming. Ni catalysts are known to be highly active for the chemisorption of organothiols [1]. The adsorption of *n*-alkanethiols on metal surfaces such as gold and nickel was found to be highly ordered and leads to structurally well-defined organic monolayers [20–22].

In the present work, we have studied the effects of contamination of Ni catalyst with *n*-alkanethiols (H–$(CH_2)_n$–SH, $n = 4$, 5, 6 and 10) on the catalyst activity during steam reforming of methane for a CH_4:H_2O ratio 1:2. We have previously shown that under these conditions and with this feedgas ratio the unsupported Ni catalyst exhibited high catalytic activity (CH_4 conversion = 98 ± 2% at $T = 700\,^{\circ}C$), no coke deposition, long-term stability during the steam reforming of methane at low–medium temperature range, and the system is close to thermodynamic equilibrium [23,24]. The thiol-contaminated Ni catalysts are denoted herein as Ni–C_nS where $n = 4$, 5, 6 and 10. Rather than subject the catalysts to long-term low-level thiol contaminations as might be found in commercial feedgas systems, this study employed accelerated determination of the effects of thiol contamination by examining surfaces that are pre-saturated with the chemisorbed thiol-bearing organic phase. The thiol-contaminated Ni catalyst powders were prepared by extended immersion of pristine Ni catalyst powder in a solution of *n*-alkanethiol/methanol with continual agitation. The initial chemisorption of *n*-alkanethiol on Ni catalysts was confirmed using infrared spectroscopy (IR) and X-ray photoemission spectroscopy (XPS). The coke formation and sulfur content were determined using XPS analysis. Short chain thiol-contaminated Ni catalysts, Ni–C_4S and Ni–C_5S, were the most stable contaminated catalysts with respect to deactivation. However, Ni–C_6S and Ni–$C_{10}S$ exhibited rapid and irreversible deactivation during steam reforming of methane. In these cases, the catalysts' deactivation was found to be due to aromatic carbon deposition.

2. Materials and methods

2.1. Sample preparation

The unsupported Ni catalyst used in this study is a pure nickel powder ($S_{BET} = 0.44\ m^2\ g^{-1}$, particle size range of 1–20 μm) with an open filamentary structure and irregular spiky surface. It is produced by the thermal decomposition of nickel tetracarbonyl [25] and is supplied by Inco (Inco Ni 255). More details about this product can be found elsewhere [23].

The normal alkanethiols considered in this work are H–$(CH_2)_n$–SH, with $n = 4$, 5, 6 and 10. They are all liquids at room temperature and were used as received: *n*-decanethiol (Aldrich, 98%), *n*-hexanethiol (Aldrich, 98%), *n*-pentanethiol (Aldrich, 99%), and *n*-butanethiol (Aldrich, 99%). Methanol solvents (Aldrich, 99%) were also used as received.

The thiol contamination of Ni catalyst was obtained by immersion of the pristine nickel powder in 10^{-3} M solutions of alkanethiols/methanol (5 g of Ni in 100 ml of solution) at room temperature; these solutions contained several orders of magnitude excess thiol as compared to the monolayer quantities. The immersion time was 20 h. After immersion, all such treated samples were rinsed in copious quantities of fresh methanol. Finally, the samples were dried for 12 h at ambient temperature and then used for characterization and reforming tests. Comparison of the reforming activity measured using Ni samples that were pre-reduced under flowing H_2/Ar and with non-reduced Ni powders showed no significant differences, presumably because of the abundance of hydrogen available to the Ni surfaces during normal reforming processes.

2.2. Experimental set-up and protocol for catalytic activity measurement

The catalytic activity measurements were conducted at atmospheric pressure in a seven-cell differential reactor system that was constructed for real-time monitoring of the reforming reaction (Fig. 1). The experimental set-up is equipped with a gas humidification system, a programmable furnace and a

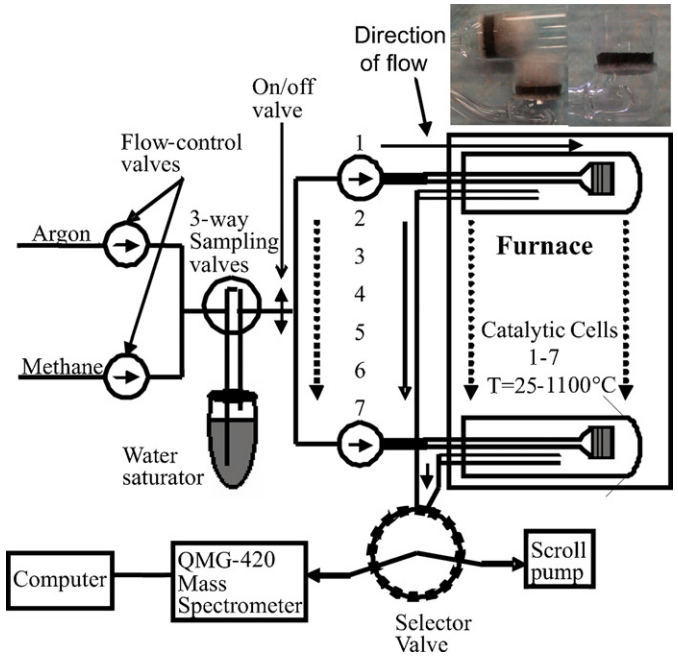

Fig. 1. Schematic view of the multicell reformer evaluation bench.

quadrupole mass spectrometer (Balzers QMG-420). The reactant gas is composed of CH_4 (Praxair, Ultra high purity), Ar (Praxair, Ultra high purity) and steam. The partial pressure of water in the gas is used to regulate the CH_4:H_2O ratio; it is fixed by controlling the temperature of the water through which the reaction gas was bubbled. The reaction gas was distributed equally among the seven quartz reaction chambers such that different catalysts could be tested simultaneously under identical reaction conditions. The gas compositions and flow rates are controlled by rotameters (OMEGA). The flow rate used was 25 ml min^{-1} per tube. The 0.25 g of catalyst is lightly packed into the inner quartz tubes and retained by quartz wool. The inner tubes include porous fused quartz disks (coarse porosity of 40–90 μm, 1.5 cm diameter) that supported the Ni catalyst beds (photo in Fig. 1). No entrainment of catalyst particles occurs downstream because the catalyst pellet is already lightly compressed and during the early stages of the catalytic reaction there is sufficient sintering to preserve the structural integrity of the pellet. The mass-stability of the catalyst bed has been directly confirmed gravimetrically. The product gases from each reactor cell were sampled in a round-robin sequence using a computer-controlled valve assembly (Valco) and directed to the mass spectrometer for identification. The mass selected intensities were calibrated using pure standard gases diluted in the Ar carrier gas. The overall measurement accuracy is ±3% and the reproducibility is ±2%. In each experiment the furnace temperature was increased at a constant rate of 3 °C min^{-1}. The temperatures reported herein were measured in the free-volume of the furnace system with a type K thermocouple that is independent of the temperature control system. The measurement of the temperature at the surface of the catalyst was tested to determine if the endothermic nature of the reforming reaction caused significant cooling of the active surface. A thermocouple is placed on the surface of the Ni catalyst and another on the surface of the porous fused quartz disk. The temperatures at these two places measured during these tests were equal or higher by 12 ± 2 °C than those measured in the free-space of the oven when the temperature in the latter is kept at 700 °C. The differences among these temperatures inside the oven are due to uneven radiation emissivities and non-homogeneous convection current profiles.

In this study, for each experiment, we tested at least two samples, and the CH_4 conversion is defined as follows:

$$CH_4 \text{ conversion } (\%) = \left(\frac{(P_{\text{in},CH_4} - P_{\text{out},CH_4})}{P_{\text{in},CH_4}} \right) \times 100\%$$

2.3. Catalyst characterization

Diffuse reflectance infrared Fourier transform spectroscopy (DRIFTS) was used to characterize the Ni powder using a Nicolet Nexus 470 FT-IR spectrometer. The resolution was 4 cm^{-1} and 256 scans were accumulated in an inert atmosphere at room temperature. The spectra were acquired using a MCT detector. The DRIFTS results presented in this work are based on the frequencies and absolute intensities of the absorption bands in the "high-frequency" C–H stretching region (2800–3000 cm^{-1}).

X-ray photoelectron spectra (XPS) for catalyst samples were acquired at room temperature using a Kratos HS system with a monochromatized Al K_α ($h\nu$ = 1486.6 eV) X-ray source operated at 120 W; a 12000 μm^2 region of the sample was probed. The samples were introduced and maintained at room temperature throughout the measurements. The photoelectron kinetic energies were measured using a hemispherical electrostatic analyzer working in the constant pass energy mode. The background pressure in the analyzing chamber was below 2×10^{-8} Torr. Survey scans (0–1200 eV) and high-resolution Ni 3p, S 2p, C 1s and O 1s spectra were obtained at pass energy of 160 and 40 eV, respectively. Correction for charging effects was achieved by referencing all binding energies with respect to the O 1s core level spectrum in NiO (BE ≈ 529.1 eV [26]). The uncertainty in peak position was estimated to be ±0.2 eV for all spectra. The analysis of the measured Ni 3p, S 2p, C 1s and O 1s high-resolution spectra envelopes was performed by curve-fitting synthetic peak components using XPSPEAK41. The raw experimental data were used with no preliminary smoothing. Gaussian–Lorentzian product functions and Shirley background subtraction procedures were used to approximate the line shapes of the fitting components. Quantification of the sulfur and carbon atomic percentages was obtained from integration of the S 2p and C 1s core-level spectra with the appropriate corrections for photo-ionization cross-sections.

3. Results

Fig. 2 shows the DRIFTS results and the assignments of the various bands for various *n*-alkanethiols adsorbed on the Ni powder at ambient temperature. The data show the presence of the diagnostic C–H stretching bands as characterized by (i) the d^+ band (~2850 cm^{-1}), associated with the symmetric

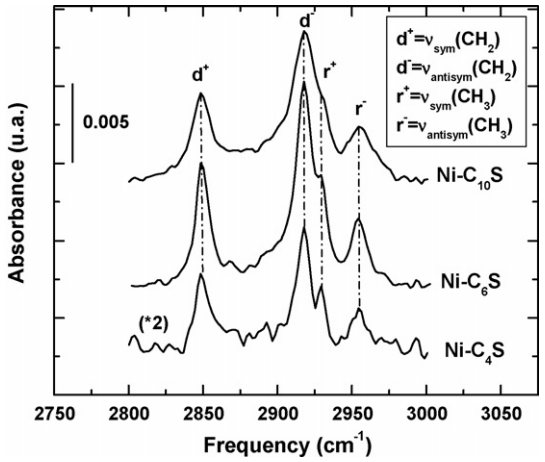

Fig. 2. DRIFTS spectra of the as-prepared thiol-contaminated Ni catalysts.

vibration of the CH_2 units of the backbone chain, (ii) the d^- band ($\sim$2918 cm^{-1}), associated with the antisymmetric vibration of the CH_2 units of the backbone chain, (iii) the Fermi-resonance influenced r^+_{FR} band ($\sim$2930 cm^{-1}), associated with symmetric vibrations of the terminal CH_3 groups, and (iv) the r^- band ($\sim$2955 cm^{-1}), associated with antisymmetric vibrations of the terminal CH_3 groups) [21,27]. The relative intensities of these various bands, their peak positions, and the peaks widths are remarkably similar to those of the alkanethiol monolayers adsorbed on planar Au(1 1 1) substrates [21,27], suggesting that the local environment of these adsorbates on the Ni surface is rather well ordered, despite the long-range disorder implicit in the use of powdered surfaces. None of the spectra of the thiol-contaminated Ni powders exhibited significant intensity on the r^+ band ($\sim$2875 cm^{-1}) that is associated with the symmetric stretching mode of the terminal methyl groups.

Fig. 3a and b shows the XPS spectra of the C 1s and S 2p binding energy regions, respectively, for the different thiol-contaminated Ni catalyst powders, Ni–C_4S, Ni–C_5S, Ni–C_6S, and Ni–C_{10}S. From the analysis of the near-surface atom compositions for all samples, the existence of two forms of carbon C 1s located at ≈284.5 and ≈288.7 eV was detected. Table 1 provides a compilation of the energy assignments of the spectral components in all analyzed high-resolution XPS data. The peak located at ≈288.7 eV for all thiol-contaminated Ni catalysts was attributed to C=O. This originates from the Ni catalyst powder, which was commercially produced by the thermal decomposition of $Ni(CO)_4$ [25]. It is not known at this time if the residual chemisorbed CO affects the binding of the thiols to the Ni powders. The peak observed at ≈284.5 eV is attributed to graphitic (i.e. aliphatic) carbon originated from the *n*-alkanethiol molecule chemisorbed on the catalyst surface. This assignment is consistent with adsorbed thiolate [28–30].

Table 1
Energies and assignments of the XPS C 1s and S 2p spectral components and the area ratio of total sulfur on Ni calculated for the as-prepared thiol-contaminated Ni catalysts

Sample	Binding energies (eV), C 1s		Binding energies (eV), S 2p		S_{total}/Ni (%)
	Graphitic	C=O	Sulfonates	Thiolates	
Ni–C_4S	284.5	288.7	168.0	–	3.0
Ni–C_5S	284.4	288.7	168.2	–	3.6
Ni–C_6S	284.7	288.7	168.0	–	5.3
Ni–C_{10}S	284.5	288.7	168.0	162.7	10.9

In the case of sulfur S 2p spectral region (Fig. 3b), two peaks can be distinguished at 162.7 and 168 eV. The first peak corresponds to thiolates [28,30,31] and was observed only for contaminated Ni catalyst Ni–C_{10}S. The second peak, which is typical for sulfonates [31,32], was observed for all thiol-contaminated Ni catalysts. This is in good agreement with findings obtained in a study of wetting properties for self-assembled monolayers of *n*-alkanethiols on copper surfaces, which revealed that the rate of substrate oxidation decreases with increasing chain length [33]. The reduced oxygen transport to the substrates for long-chain adsorbates explains the presence of adsorbed thiolates only for Ni–C_{10}S catalyst powder. The presence of two sulfur chemical states, thiolates and sulfonates, on the catalyst surface along with the CH_2 and CH_3 stretching bands (characterized by infrared spectroscopy as described above), shows that the room-temperature adsorption of the *n*-alkanethiols takes place

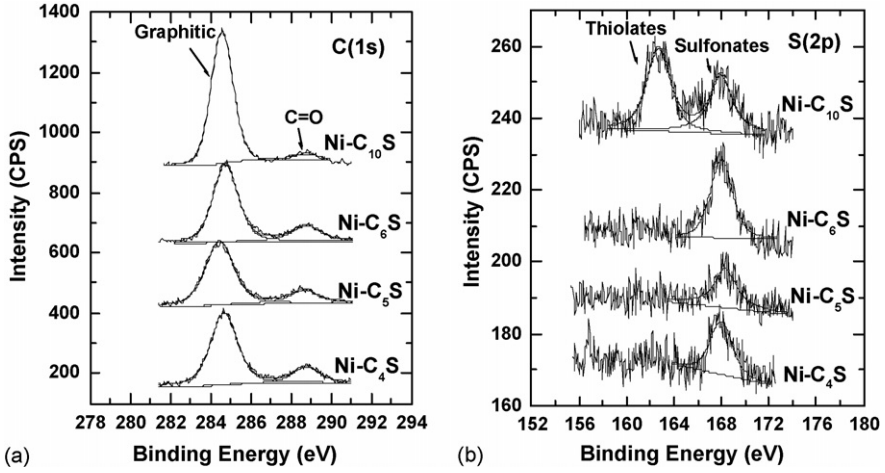

Fig. 3. XPS spectra: (a) carbon C 1s and (b) sulfur S 2p of Ni–C_4S, Ni–C_5S, Ni–C_6S, and Ni–C_{10}S catalysts.

through the sulfur atom and not through the carbonaceous chain. Table 1 provides also the relative intensities of the total sulfur with respect to the total Ni in the different thiol-contaminated Ni catalysts. The coverage ratio of the Ni by the sulfur increases with the chain length of the alkanethiol molecule, i.e. this coverage is 3% for Ni–C_4S and 10.9% for Ni–$C_{10}S$. This implies that the longer chain species lead to a higher number density of adsorbates alkanethiol molecules on the Ni powder surfaces. Mekhalif et al. [32] have reported similar results in the adsorption of *n*-alkanethiols on polycrystalline Ni substrates. Our XPS results corroborate the DRIFTS results and confirm the adsorption of the different *n*-alkanethiols on the catalyst surface by the terminal S site.

The catalytic activity of the thiol-contaminated Ni catalysts, Ni–C_4S, Ni–C_5S, Ni–C_6S and Ni–$C_{10}S$, was tested for steam reforming of methane ($CH_4 + 2H_2O \rightarrow CO_2 + 4H_2$; $CH_4 + H_2O \rightarrow CO + 3H_2$) and was compared to that of a pristine Ni catalyst. Based on our previous work [23,24], the reforming tests were conducted at a CH_4/H_2O ratio of 1:2 to ensure chemical equilibrium and high conversion yields, while avoiding any limitations related to the reaction kinetics. Fig. 4 shows the activity changes for a pristine Ni catalyst depending on time and temperature by following the partial pressures of H_2, CO, CO_2 and CH_4. The onset of hydrogen production is approximately 325 °C; H_2 production increases as temperature increases, and the maximum yield was obtained at 500 °C. As the temperature was increased from 500 to 700 °C, hydrogen production was constant, and remained stable for over 13 h at $T = 700$ °C. The relative yields of CO and CO_2 are in good agreement with a fully equilibrated thermodynamic model of the system, as shown in Fig. 6 of Ref. [24]. This suggests that under the present operating conditions, the system is controlled by thermodynamic parameters, rather than kinetic limitations. Fig. 5 shows the activity changes for the thiol-contaminated Ni catalysts Ni–C_4S, Ni–C_5S, Ni–C_6S and Ni–$C_{10}S$ depending on time and temperature. Ni–C_4S and Ni–C_5S catalysts (Fig. 5a and b) were active at relatively low temperatures 400 °C < T < 700 °C. The hydrogen

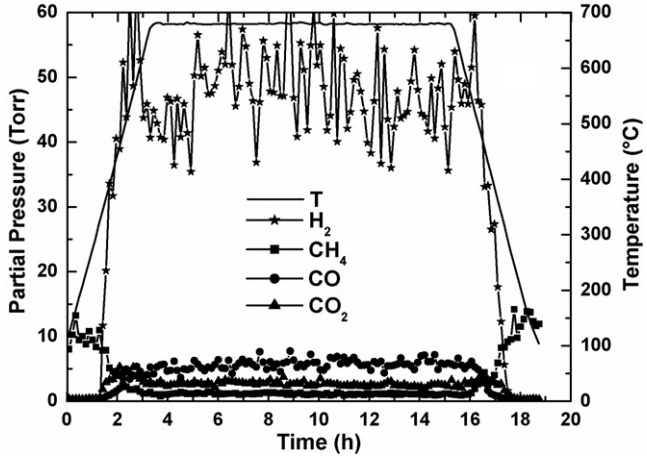

Fig. 4. Gas composition and temperature profiles vs. time on-stream for steam reforming with an unsupported Ni catalyst. Reaction conditions: $P(CH_4) = 10$ Torr, $P(H_2O) = 20$ Torr, and $P(Ar) = 730$ Torr.

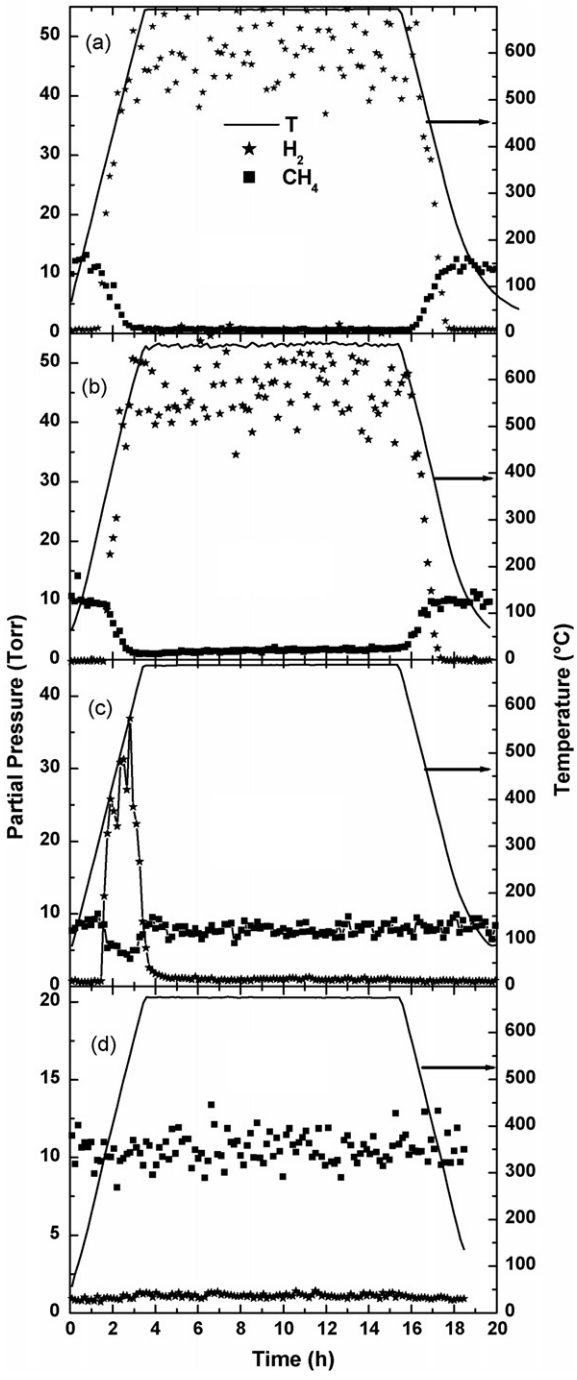

Fig. 5. Gas composition and temperature profiles vs. time on-stream for steam reforming with (a) Ni–C_4S, (b) Ni–C_5S, (c) Ni–C_6S, and (d) Ni–$C_{10}S$ catalysts. Reaction conditions: $P(CH_4) = 10$ Torr, $P(H_2O) = 20$ Torr, and $P(Ar) = 730$ Torr.

production increased as the temperature increased. The onset of hydrogen production was approximately at 325 °C with the maximum obtained at 500 °C, as was found for the pristine Ni catalysts. The production of H_2 was stable over the 20 h experiment duration as the temperature was stabilized at $T = 700$ °C; the apparent noise shown in the yield curves (and most evident in the H_2 measurements) is due to the rapid switching of selector valve between samples, and does not reflect instabilities of the catalyst performance or kinetic oscillations of the system.

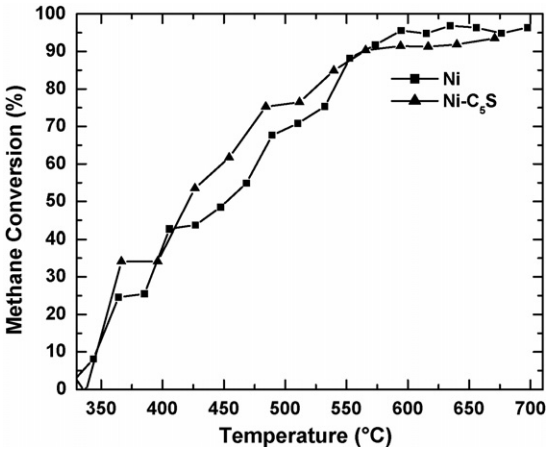

Fig. 6. Methane conversion over pristine Ni and Ni–C_5S catalysts as a function of temperature. Reaction conditions: $P(CH_4) = 10$ Torr, $P(H_2O) = 20$ Torr, and $P(Ar) = 730$ Torr.

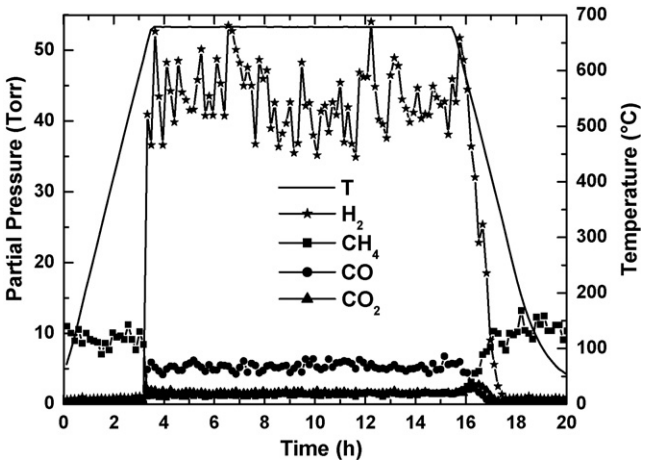

Fig. 8. Gas composition and temperature profiles vs. time on-stream in steam reforming tests preceded by thermal treatment of the unsupported Ni catalyst at 700 °C. Reaction conditions: $P(CH_4) = 10$ Torr, $P(H_2O) = 20$ Torr, and $P(Ar) = 730$ Torr.

The methane conversion over Ni–C_5S catalysts was $94 \pm 2\%$ (Fig. 6). At the same conditions this percentage was $97 \pm 2\%$ over pristine Ni catalyst (Fig. 6), indicating that the loss of catalytic activity of Ni–C_5S was negligible (Fig. 4). In the case of the Ni–C_6S catalyst an abrupt decrease of the catalytic activity was observed when the temperature exceeded ~580 °C. Above this temperature, the catalyst was completely deactivated. The decrease of catalytic activity is irreversible with temperature. No catalytic activity was observed using the Ni–$C_{10}S$ catalyst, at any temperature (Fig. 5d).

It can be concluded that at any temperature, the catalytic activity of the thiol-contaminated Ni catalyst depends on the nature of the *n*-alkanethiol contaminant; in particular, the chain length appears to be the critical factor in determining the thiol's influence.

Typical XPS spectra in the C 1s and S 2p regions of the thiol-contaminated Ni catalysts Ni–C_4S, Ni–C_5S, Ni–C_6S, and Ni–$C_{10}S$ obtained after their use in steam reforming tests are shown in Fig. 7a and b. The XPS spectra of S 2p shows significant differences as compared to the spectra of the thiol-contaminated Ni catalysts prior to the exposure to high temperatures and the $CH_4 + H_2O$ fuel mixture (Fig. 3b). For all samples, a shift of the S 2p peak to the lower binding energies was observed; this shift is attributed to the increased abundance of thiol adsorbates (≈162.2 eV) and it was indicative of the formation of thiolate bonds with a metallic substrate [28,30,31]. The absence of sulfonates can be explained by the reduction of nickel surface by hydrogen produced during the steam reforming of methane. In the case of carbon, three components are necessary to obtain a satisfactory fit to the data. The first compound at ≈284.6 eV is assigned to a graphitic or aliphatic-like carbon. The second at a higher energy (≈288.7 eV) is assigned to C=O, and the third compound at ≈285.6 eV which could be related to an aromatic type in small compounds. Assignment of the later species was recognized through the studies of methane aromatization in membrane reactors conducted by Larachi et al. [34] and Darmstadt et al. [35]. Kane and Gland [30] through their study of

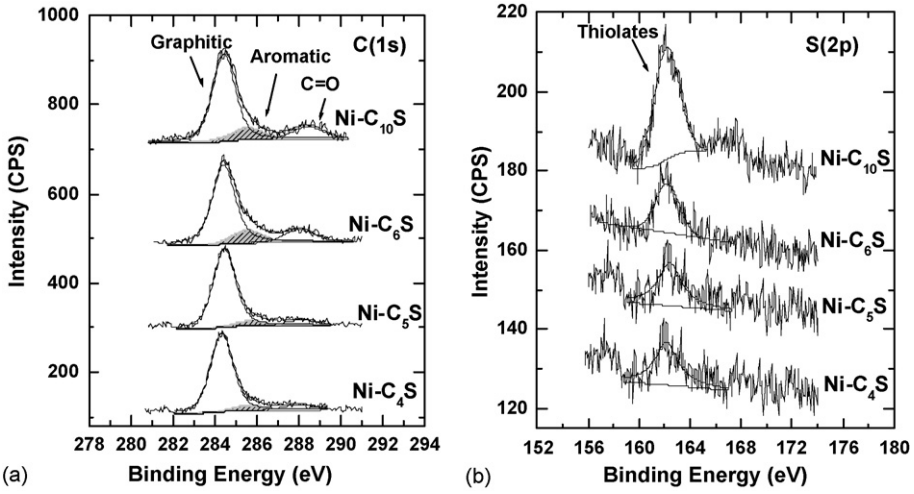

Fig. 7. XPS spectra for Ni–C_4S, Ni–C_5S, Ni–C_6S, and Ni–$C_{10}S$ catalysts measured after their use in steam reforming tests for (a) carbon C 1s and (b) sulfur S 2p. Reaction conditions: $P(CH_4) = 10$ Torr, $P(H_2O) = 20$ Torr, $P(Ar) = 730$ Torr, time of reforming = 20 h, and $T = 700$ °C for 12 h.

adsorption and reaction of cyclohexanethiol on the Ni(1 0 0) surface as a function of temperature, they have also reported the formation of aromatic carbon. This peak (BE ≈ 285.6 eV) was absent in all as-prepared thiol-contaminated Ni catalysts (Ni–C_4S, Ni–C_5S, Ni–C_6S, and Ni–C_{10}S), as shown previously in Fig. 3a.

Additional experiments were carried out to identify the cause(s) of the deactivation process of the Ni–C_4S, Ni–C_5S, Ni–C_6S, and Ni–C_{10}S catalysts. After thermal treatment of the pristine and thiol-contaminated Ni catalysts Ni–C_4S, Ni–C_5S, Ni–C_6S, and Ni–C_{10}S at 700 °C under to a pure Ar carrier gas (25 ml min^{-1}), the catalytic activity was tested for the steam reforming of methane for CH_4:H_2O ratio of 1:2. Fig. 8 shows the catalytic activity for pristine Ni catalysts by following the partial pressures of H_2, CO, CO_2 and CH_4 during the same temperature ramp that was used in previous reforming experiments. The onset of hydrogen production is approximately 630 °C, and, at this temperature, the maximum yield was identical to that of the pristine Ni catalysts tested without the Ar pretreatment. From 630 to 700 °C, hydrogen production was stable during time. The increased temperature for the onset of H_2 production, relative to catalysts that have no been exposed to the high-temperature Ar carriers gas (e.g. the data of Fig. 4), appears to be due to the slightly reduced activity due to the sintering of the loose Ni powder to create the porous solid. In all other respects, the Ar pretreatment has no effect on the catalytic properties of the pristine Ni samples. Fig. 9a and b show that the onset for H_2 production using the Ar-pretreated Ni–C_4S and Ni–C_5S samples is also observed at higher temperatures than for the unsintered materials (e.g. Fig. 5). More importantly, it is clear than in contrast to the results of Fig. 5, the catalytic activity of the Ni contaminated by the short chain thiols now decreases over time at 700 °C following the Ar pretreatment. For Ni–C_6S and Ni–C_{10}S, no catalytic activity was observed (Fig. 9c and d). By comparing these results to those obtained for non-contaminated Ni catalyst in similar experimental conditions (Fig. 8), it is clear that the surface bound *n*-alkanethiol molecules are responsible of the catalysts' deactivation.

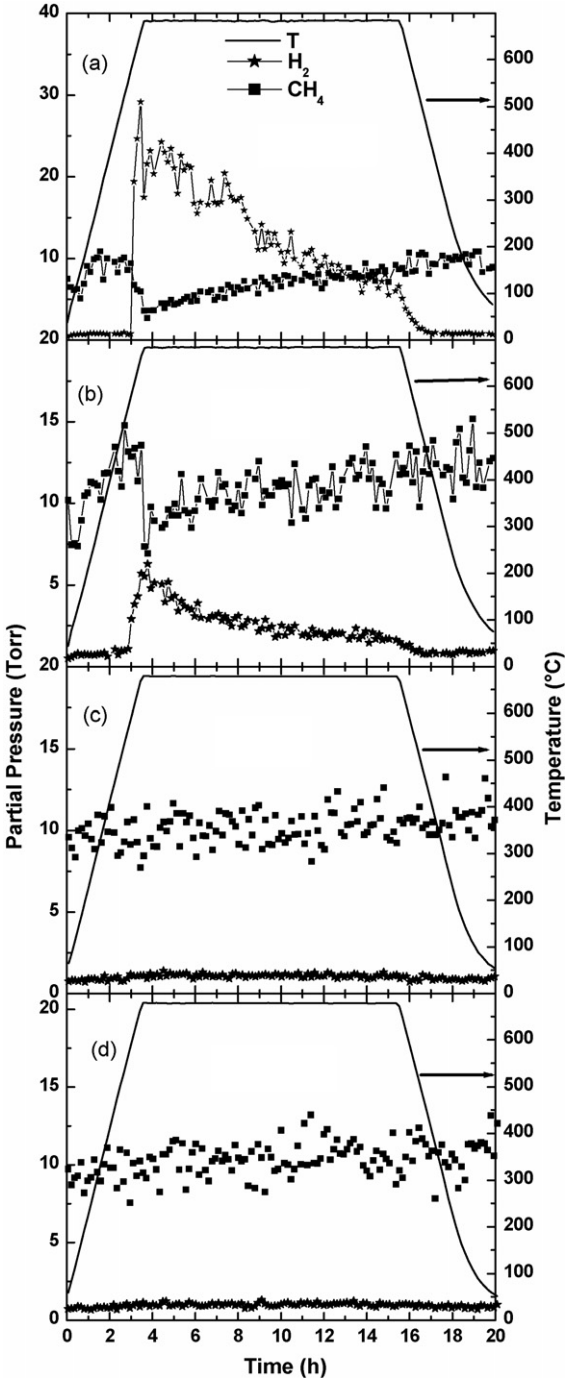

Fig. 9. Gas composition and temperature profiles vs. time on-stream in experiments preceded by thermal treatment at 700 °C of the (a) Ni–C_4S, (b) Ni–C_5S, (c) Ni–C_6S, and (d) Ni–C_{10}S catalysts. Reaction conditions: $P(CH_4)$ = 10 Torr, $P(H_2O)$ = 20 Torr, and P(Ar) = 730 Torr.

Fig. 10a and b show the XPS spectra of the C 1s and S 2p, respectively, for the thiol-contaminated Ni catalysts Ni–C_4S, Ni–C_5S, Ni–C_6S, and Ni–C_{10}S, which were obtained following the steam reforming of methane and the Ar pretreatment at 700 °C. As can be seen from Figs. 10 and 7, a similar behavior was observed for all samples indicating the presence of graphitic-like carbon (BE ≈ 284.4 eV), the C=O (BE ≈ 288.2 eV), an aromatic-aliphatic carbon (BE ≈ 285.6 eV), and thiolates (BE ≈ 162.2 eV).

4. Discussion

A determination of the chemical species responsible of the observed deactivation of the thiol-contaminated Ni catalyst for chain lengths greater than C_5 is made using the XPS data shown in Figs. 3, 7 and 10. Table 2 provides the relative intensities of aromatic carbon and the total sulfur with respect to the total Ni for thiol-contaminated Ni catalysts Ni–C_4S, Ni–C_5S, Ni–C_6S, and Ni–C_{10}S, obtained after: (a) the as-prepared thiol-contaminated Ni catalysts, (b) their use in the steam reforming tests, and (c) their use in the steam reforming test preceded by thermal treatment under Ar carrier gas at 700 °C. The percentage of the Ni surface coverage by sulfur (S/Ni × 100) for all thiol-contaminated Ni catalysts after their use in steam reforming tests is significantly different from those of the as-prepared thiol-contaminated Ni catalysts (Table 2). For each sample, the S/Ni ratio decreased following use in steam reforming and continue to decrease in advantage following use in the steam reforming test

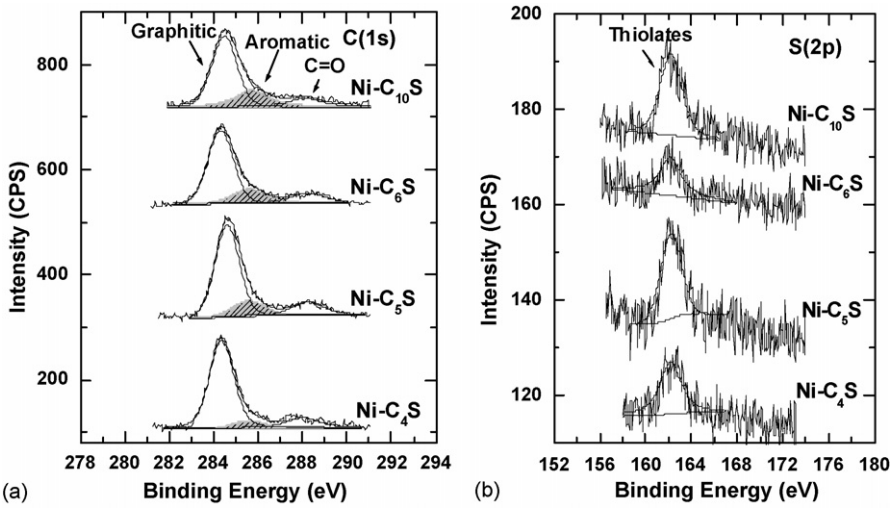

Fig. 10. XPS spectra for (a) C 1s and (b) S 2p of thiol-contaminated Ni catalysts Ni–C_4S, Ni–C_5S, Ni–C_6S, and Ni–$C_{10}S$ obtained after their use in steam reforming test preceded by thermal treatment under Ar carrier gas at 700 °C). Reaction conditions: $P(CH_4) = 10$ Torr, $P(H_2O) = 20$ Torr, $P(Ar) = 730$ Torr, $T = 700$ °C for 12 h.

preceded by thermal treatment under Ar carrier gas at 700 °C. In addition, Table 2 shows also that the quantity of aromatic carbon detected was greater for each thiol-contaminated Ni catalyst when the reforming operation was preceded by the extended Ar exposure at high temperatures. Specifically, the quantity of adsorbed aromatic carbon increased by at least 50% for Ni–C_4S and Ni–C_5S, and by about 10% for Ni–C_6S and Ni–$C_{10}S$, as a result of the Ar pretreatment, while there is no adsorption of aromatic carbon for the as-prepared thiol-contaminated Ni catalysts. Similarly, Table 2 shows that the quantity of aromatic carbon for the thiol-contaminated Ni catalysts measured after their use in steam reforming test increased with the length of the alkyl chain.

Based on the above results, the observed deactivation of Ni–C_6S and Ni–$C_{10}S$ during the steam reforming of methane may be due to (a) the deposition of significant amount of aromatic carbon on the catalyst surface, and/or (b) to a permanent poisoning of the surface caused by the high level of chemisorbed sulfur species.

We note that the percentage of the Ni surface coverage by sulfur (S/Ni × 100) for Ni–C_5S obtained after its use in steam reforming test (2.7%) is essentially similar to that of the Ni–C_6S following use in the steam reforming test preceded by thermal treatment under Ar carrier gas at 700 °C (2.6%). The fact that in those conditions Ni–C_6S deactivate and Ni–C_5S remains active confirms that sulfur is not responsible of the catalyst deactivation. In addition, despite the reduced S content, the catalytic activity of the Ni–C_4S and Ni–C_5S samples exhibit reduced catalytic activity following the Ar pretreatment; these findings suggest that the loss of catalytic activity, observed for the thiol-contaminated Ni samples, is indeed due to the accumulation of higher amounts of aromatic carbon on the surfaces.

Rostrup-Nielsen et al. [7] have reported that operation with feed gases containing substantial amounts of higher hydrocarbons may cause a problem for a sulfur passivity process, because these hydrocarbons may crack thermally into olefins, which may form pyrolytic carbon. Another study [3] has shown that the formation of coke on oxides and sulfides is principally a result of cracking reactions involving coke precursors (typically olefins or aromatics) catalyzed by acid sites. Aromatic carbon can also be produced by methane aromatization [34,36]. For this study, to better understand the phenomena of the formation of aromatic carbon and to identify which molecule (i.e. the pre-adsorbed alkanethiols or feed-gas methane) was responsible for its formation, a 2 h, 700 °C exposure to flowing Ar was carried out without exposure of the samples to the reforming feed gas, and an XPS analysis of the carbon and sulfur was performed. Inspection of the C 1s and S 2p levels for the four types of substrates (Fig. 11a and b) revealed the familiar three peaks of the C 1s located at ≈284.4, ≈285.6, and ≈288.1 eV; as before, these are attributed to graphitic-like carbon, an aromatic-aliphatic carbon and C=O, respectively. The absence of methane in the experimental conditions and the presence of the peak located at 285.6 eV, which is not present in non contaminated Ni catalyst (Fig. 11a), prove that

Table 2
Area ratio of aromatic carbon and the total sulfur on Ni calculated for the thiol-contaminated Ni catalysts Ni–C_4S, Ni–C_5S and Ni–C_6S measured after: (a) the as-prepared thiol-contaminated Ni catalysts; (b) their use in the steam reforming tests (CH_4:H_2O = 1:2, P_{total} = 1 atm, time of reforming = 20 h, and T = 700 °C for 12 h); (c) their use in the steam reforming test preceded by thermal treatment under Ar carrier gas at 700 °C (CH_4:H_2O = 1:2, P_{total} = 1 atm, time of reforming = 20 h, and T = 700 °C for 12 h)

	Ni–C_4S $C_{aromatic}$/Ni (%)	Ni–C_5S $C_{aromatic}$/Ni (%)	Ni–C_6S $C_{aromatic}$/Ni (%)	Ni–$C_{10}S$ $C_{aromatic}$/Ni (%)	Ni–C_4S S_{total}/Ni (%)	Ni–C_5S S_{total}/Ni (%)	Ni–C_6S S_{total}/Ni (%)	Ni–$C_{10}S$ S_{total}/Ni (%)
(a)	–	–	–	–	3.0	3.6	5.3	10.9
(b)	3.0	4.0	6.8	10.1	2.4	2.7	3.1	5.1
(c)	5.0	6.1	7.5	11	2.1	2.5	2.6	4.0

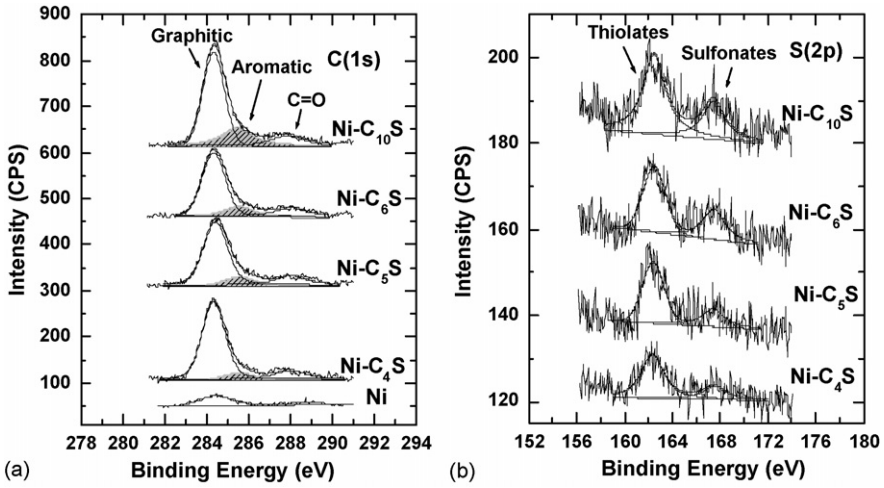

Fig. 11. XPS spectra for (a) C 1s and (b) S 2p of Ni–C_4S, Ni–C_5S, Ni–C_6S, and Ni–$C_{10}S$ catalysts measured after their thermal treatment under Ar carrier gas at 700 °C for 2 h.

the formation of aromatic-aliphatic carbon was due to the pyrolysis of the *n*-alkanethiols pre-adsorbed on the catalyst surface, and not from the feed gas (methane). The S 2p results (Fig. 11b) consistently exhibit two peaks located at ≈162.4 and ≈167.5 eV, corresponding to thiolate and sulfonate species, respectively. Recalling that the Ni–C_4S, Ni–C_5S and Ni–C_6S samples did not exhibit the thiolate peaks prior to heating (e.g. Fig. 3), this result shows that the nickel-organic interface was partially reduced during the Ar pretreatment. Table 3 provides the relative intensities of aromatic carbon and sulfur (with respect to the total Ni) for the thiol-contaminated Ni catalysts Ni–C_4S, Ni–C_5S, Ni–C_6S, and Ni–$C_{10}S$ obtained after the Ar-exposure test. In each case, the area coverage percentages of aromatic carbon and sulfur were virtually identical to those reported for thiol-contaminated Ni catalysts measured after their use in steam reforming test (e.g. Table 2). These results confirm that the formation of aromatic carbon is due to the degradation of the *n*-alkanethiols pre-adsorbed on the nickel surfaces.

The area coverage percentage of aromatic carbon in thiol-contaminated Ni catalysts Ni–C_4S, Ni–C_5S, Ni–C_6S, and Ni–$C_{10}S$ obtained after their use in steam reforming test (e.g. Table 2) correlates closely with the degree of deactivation for the steam reforming of methane reaction. These results suggest that the quantity of aromatic carbon formed on the catalyst surface is the key parameter in deactivation. To estimate the levels of the aromatic carbon that lead to the deactivation of catalysts surface, steam reforming of methane for three catalytic tests over thiol-contaminated Ni catalyst Ni–C_6S were carried out with temperature ramps up to 400, 580, and 700 °C. The selected temperatures represent the onset, the maximum, and the higher temperature of the production of hydrogen, respectively, for the Ni–C_6S samples (e.g. Fig. 5c). Following the reforming tests, the used Ni–C_6S samples were analyzed with XPS and the results are presented in Fig. 12; the relative intensities of aromatic carbon (C/Ni ratios) are presented in Table 4 for each temperature selected. The results show that ∼80% of the aromatic carbon is formed as the samples are heated to 400 °C, with a further ∼10–20% as the maximum temperature increases to 580 °C and 700 °C respectively. The Ni–C_6S catalyst was deactivated as the temperature exceeded ∼580 °C and at this temperature the area coverage percentage of aromatic carbon was 4.6%. We therefore estimate that this is the threshold for significant surface deactivation under the conditions of our experiments. It is interesting to note that the catalytic activity is a strongly non-linear function of the aromatic carbon content of the surface. Zeuthen et al. [37] have demonstrated that the presence of aromatic-type coke

Table 3
Area ratio of aromatic carbon and the total sulfur on Ni calculated for the as-prepared thiol-contaminated Ni catalysts measured after Ar pretreatment at 700 °C for 2 h

Sample	$C_{aromatic}$/Ni (%)	S_{total}/Ni (%)
Ni–C_4S	3.0	2.4
Ni–C_5S	4.1	2.6
Ni–C_6S	6.9	3.3
Ni–$C_{10}S$	10.1	5.1

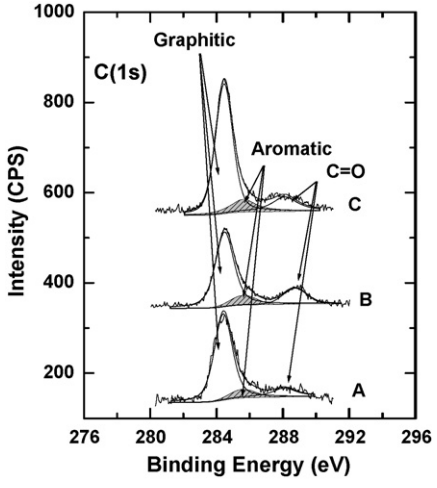

Fig. 12. XPS C 1s spectra of thiol-contaminated Ni catalyst Ni–C_6S obtained after its uses in steam reforming test up to a temperature of (A) 400 °C, (B) 580 °C, and (C) 700 °C. $P(CH_4)$ = 10 Torr, $P(H_2O)$ = 20 Torr, and $P(Ar)$ = 730 Torr.

Table 4
Area ratio of aromatic carbon on Ni calculated for Ni–C_6S catalyst measured after use in the steam reforming test for several maximum temperatures (CH_4:H_2O = 1:2, P_{total} = 1 atm)

Sample	Temperature (°C)	$C_{aromatic}$/Ni (%)
Ni–C_6S	400	4.2
Ni–C_6S	580	4.6
Ni–C_6S	700	5.2

at levels above 5% causes deactivation of Ni–Mo catalysts. The close similarity to the results presented herein suggests that this level of surface coverage by aromatic carbons is a robust indicator of the surface activity for Ni-based material.

5. Conclusion

An unsupported Ni catalyst has been contaminated with *n*-alkanethiols (*n*-C_4H_9-SH, *n*-C_5H_{11}-SH, *n*-C_6H_{13}-SH and *n*-$C_{10}H_{21}$-SH) and the catalytic activity of the samples was determined for steam reforming of methane at a CH_4:H_2O ratio of 1:2. Using XPS and DRIFTS methods it is shown that the adsorption of the *n*-alkanethiol molecules takes place through the sulfur atom. Furthermore, the longer alkyl chain species lead to increased surface coverage on the catalyst. The catalytic activity of the Ni–C_4S, Ni–C_5S, Ni–C_6S and Ni–$C_{10}S$ catalysts depends on the alkyl chain lengths. The experimental results show that the catalytic activities of Ni–C_4S and Ni–C_5S are similar to those obtained with non-contaminated Ni catalysts, with high methane conversions and high stability over the 12 h reforming reactions. It has been also shown that the adsorption of *n*-C_6H_{13}–SH on unsupported Ni catalysts causes a dramatic decrease in the catalytic properties as the temperature exceeded ~580 °C. Above this temperature, the Ni–C_6S catalysts were completely deactivated. For Ni–$C_{10}S$, no catalytic activity was obtained at any temperature. The deactivation of the unsupported Ni catalysts is mainly due to the presence of high coverage of the catalyst surface by aromatic-aliphatic carbon. The formation of aromatic-aliphatic carbon during steam reforming was found to be due to the pyrolysis of carbon from *n*-alkanethiols preadsorbed on the catalyst surface and not from the methane feed gas, with longer chain contaminants leading to more rapid accumulation of the aromatic carbon and more rapid deactivation. A Ni surface area coverage by aromatic carbon of over 4.6% leads to complete deactivation of Ni catalyst surface. Thus, unsupported Ni is a promising catalyst for robust steam reforming of natural gas containing short chain alkanethiols ($n < 6$). Work in progress is determining the long-term stability of these contaminated catalysts, and will be reported separately.

Acknowledgements

We gratefully acknowledge the financial support of this work by NSERC (Natural Sciences and Engineering Research Council) and CFI (Canadian Foundation for Innovation). We thank Sonia Blais for her assistance in the XPS measurements.

References

[1] J.R. Rostrup-Nielsen, J. Sehested, J.K. Nørskov, Adv. Catal. 47 (2002) 65.
[2] H.S. Bengaard, J.K. Nørskov, J. Sehested, B.S. Clausen, L.P. Nielsen, A.M. Molenbroek, J.R. Rostrup-Nielsen, J. Catal. 209 (2002) 365.
[3] C.H. Bartholomew, Appl. Catal. A: Gen. 212 (2001) 17.
[4] P. Forzatti, L. Lietti, Catal. Today 52 (1999) 165.
[5] D.L. Trimm, Catal. Today 49 (1999) 3.
[6] D.L. Trimm, Catal. Today 37 (1997) 233.
[7] J.R. Rostrup-Nielsen, Catalytic steam reforming, in: J.R. Anderson, M. Boudart (Eds.), Catalysis, Science and Technology, vol. 5, Sprimger-Verlag, Berlin, 1984 (Chapter 1).
[8] J.R. Rostrup-Nielsen, J. Catal. 33 (1974) 184.
[9] J.R. Rostrup-Nielsen, J. Catal. 85 (1984) 31.
[10] C.H. Bartholomew, P.K. Agrawal, J.R. Katzer, Adv. Catal. 31 (1983) 135.
[11] J. Zhen, J.J. Strohm, C. Song, Prep. Symp. Am. Chem. Soc., Div. Fuel Chem. 48 (2) (2003) 750.
[12] I.I. Novochinskii, C.S. Song, X. Ma, X.S. Liu, L. Shore, J. Lampert, R.J. Farrauto, Energy Fuels 18 (2004) 576.
[13] J. Oudar, Catal. Rev. Sci. Eng. 22 (1980) 171.
[14] L.L. Hegedus, R.W. McCabe, Catal. Rev. Sci. Eng. 23 (1981) 377.
[15] M. Salmeron, G.A. Somorjai, R.R. Chianelli, Surf. Sci. 127 (1983) 526.
[16] J.R. Rostrup-Nielsen, J. Catal. 11 (1968) 220.
[17] C.H. Bartholomew, G.D. Weatherbee, G.A. Jarvi, J. Catal. 60 (1979) 257.
[18] I. Alstrup, N.T. Andersen, J. Catal. 104 (1987) 466.
[19] Scentinel F-20 Product Literature, Chevron Phillips Chemical Company.
[20] D. Marc, T.B. Porter, D.L. Bright, C.E.D. Allara, Chidsey, J. Am. Chem. Soc. 109 (1987) 3559.
[21] K.D. Truong, P. Rowntree, J. Phys. Chem. 100 (1996) 19917.
[22] B. Parker, A.J. Gellman, Surf. Sci. 292 (1993) 223.
[23] S. Rakass, P. Rowntree, N. Abatzoglou, Proceedings of Science in Thermal and Chemical Biomass Conversion, Victoria Conference Center and Fairmont Hotel Victoria, Vancouver Island, BC, Canada, 30 August–2 September, 2004.
[24] S. Rakass, H. Oudghiri-Hassani, P. Rowntree, N. Abatzoglou, J. Power Sources 158 (2006) 485.
[25] F.V. Lenel, Powder Metallurgy, Principles and Applications, MPIF, Princeton, NJ, 1980, pp. 40.
[26] K.S. Kim, R.E. Davis, J. Electron Spectrosc. Related Phenomena 1 (1973) 251.
[27] C. Chung, M. Lee, J. Electroanal. Chem. 468 (1999) 91.
[28] D.R. Huntley, J. Phys. Chem. 96 (1992) 4550.
[29] T.S. Rufael, D.R. Huntley, D.R. Mullins, J.L. Gland, J. Phys. Chem. B 102 (1998) 3431.
[30] S.M. Kane, J.L. Gland, Surf. Sci. 468 (2000) 101.
[31] Z. Mekhalif, J. Riga, J.-J. Pireaux, J. Delhalle, Langmuir 13 (1997) 2285.
[32] Z. Mekhalif, F. Laffineur, N. Couturier, J. Delhalle, Langmuir 19 (2003) 637.
[33] P.E. Laibinis, G.M. Whitesides, D.L. Allara, Yu-T. Tao, A.N. Parikh, R.G. Nuzzo, J. Am. Chem. Soc. 113 (1991) 7152.
[34] F. Larachi, H. Oudghiri-Hassani, M.C. Iliuta, B.P.A. Grandjean, P.H. McBreen, Catal. Lett. 84 (3) (2002) 183.
[35] H. Darmstadt, A. Chaala, C. Roy, S. Kaliaguine, Fuel 75 (1996) 125.
[36] S. Qi, B. Yang, Catal. Today 98 (2004) 639.
[37] P. Zeuthen, J. Bartholdy, P. Wiwel, B.H. Cooper, Stud. Surf. Sci. Catal. 88 (1994) 199.